Int. Journ. of Fracture 19 (1982) 257–275. 00376-9429/82/04/0257-19$00.20/0

On an analytical-numerical procedure for the analysis of cylindrical shells with arbitrarily oriented cracks

H. V. LAKSHMINARAYANA and M. V. V. MURTHY

Structures Division, National Aeronautical Laboratory, Bangalore, India

L. S. SRINATH

Department of Mechanical Engineering, Indian Institute of Science, Bangalore, India

(Received January 18, 1981)

ABSTRACT

An analytical-numerical procedure for obtaining stress intensity factor solutions for an arbitrarily oriented crack in a long, thin circular cylindrical shell is presented. The method of analysis involves obtaining a series solution to the governing shell equation in terms of Mathieu and modified Mathieu functions by the method of separation of variables and satisfying the crack surface boundary conditions numerically using collocation. The solution is then transformed from elliptic coordinates to polar coordinates with crack tip as the origin through a Taylor series expansion and membrane and bending stress intensity factors are computed. Numerical results are presented and discussed for the pressure loading case.

1. Introduction

The determination of elastic stress intensity factors for an arbitrarily oriented crack in a long, thin, isotropic circular cylindrical shell loaded by axial tension, internal pressure, and torsional moment can be found in [1]. A perturbation analysis was carried out and closed form expressions were obtained for mode I and mode II components of membrane and bending stress intensity factors. These stress intensity factor solutions are valid over the complete range of the crack angle α and are quite accurate for small values of the curvature parameter β. However, in practice, we do encounter a number of situations where β falls far outside the valid range of the perturbation analysis. Previous work on symmetrically oriented cracks by Murthy *et al.* [2] has clearly shown that as β increases, perturbation solutions become increasingly conservative and result in gross over estimate of stress intensity factors. Therefore, there is a need to develop a method of analysis using which one can generate accurate stress intensity factors over a wide range of β.

A survey of literature on shells with cracks [2, 3] reveals that while axial and circumferential cracks in a cylindrical shell have been investigated quite extensively, work on an arbitrarily oriented crack is not so complete. The first attempt on the problem of an arbitrarily oriented crack in a cylindrical shell is due to Folias [4] but the stress intensity factors obtained are approximate. Analysis of a pressurised shell of revolution with a stress free crack that makes an arbitrary angle with a line of curvature of the middle surface has been carried out by Simmonds *et al.* [5]. First order corrections due to curvature to the mode I and mode II components of membrane stress intensity factor for a cracked plate were determined analytically. It is to be noted that this is only a partial solution to the problem, since it has been assumed that the predominant stresses are given by the membrane theory. It is

expected that the evaluation of bending stress intensity factors was given up due to the difficult algebra involved. Some experimental studies of fracture of circular tubes with angled cracks in torsion are reported in [6].

From the foregoing review, it is evident that the earlier procedures placed restriction on one or both of the parameters β and α. So we notice a need for a method which eliminates both these restrictions and permits analysis of practical problems. This in fact, is the purpose of the present work.

The objective of this paper is to present an analytical-numerical procedure for the computation of elastic stress intensity factors for an arbitrarily oriented crack in a circular cylindrical shell without placing any restriction on β. For the purpose of analysis, the shell is assumed to extend to infinity on either side of the crack. The material is assumed to be homogeneous, isotropic and linear elastic. Solution to the governing differential equation for the shell is obtained in the form of an infinite series in terms of Mathieu and modified Mathieu functions by the method of separation of variables. The crack surface boundary conditions are satisfied numerically with the aid of a digital computer using collocation. The solution which is completely determined, is then transformed by a Taylor series expansion from elliptic to polar coordinates with crack tip as the origin and membrane and bending stress intensity factors are determined. Numerical results are presented and discussed for loading by internal pressure.

2. General formulation

The configurations and loading conditions for which the present analysis is applicable are shown in Fig. 1. Before going into the details of the analytical-numerical procedure, we discuss briefly the general formulation which forms the basis for the analysis.

2.1. *Non-dimensionalization*

It is convenient to work with dimensionless physical quantities. Table 1 indicates the non-dimensionalizing procedure used. In this table the symbol σ denotes a reference stress, E is the Young's modulus of elasticity, t is the shell wall thickness and ν is the Poisson's ratio. σ is taken as uniform axial stress (axial tension), as uniform circumferential stress (internal pressure), and as uniform shear stress (torsional moment) in the shell in the absence of a crack.

2.2. *System of coordinates*

All the coordinate systems defined refer to the shell middle surface and are shown in Fig. 2. Coordinates with the dimension of length are non-dimensionalized with respect to a, the half crack length.

Two non-dimensional rectangular coordinate systems (x, y) and (X, Y) are defined with crack centre as the origin. The x and X axes are oriented along the shell axis and crack respectively. These two coordinate systems are connected by the linear relations:

$$x = X \cos\alpha + Y \sin\alpha, \tag{1}$$

$$y = -X \sin\alpha + Y \cos\alpha, \tag{2}$$

where α represents the angle of inclination of the crack to the shell axis (Fig. 1).

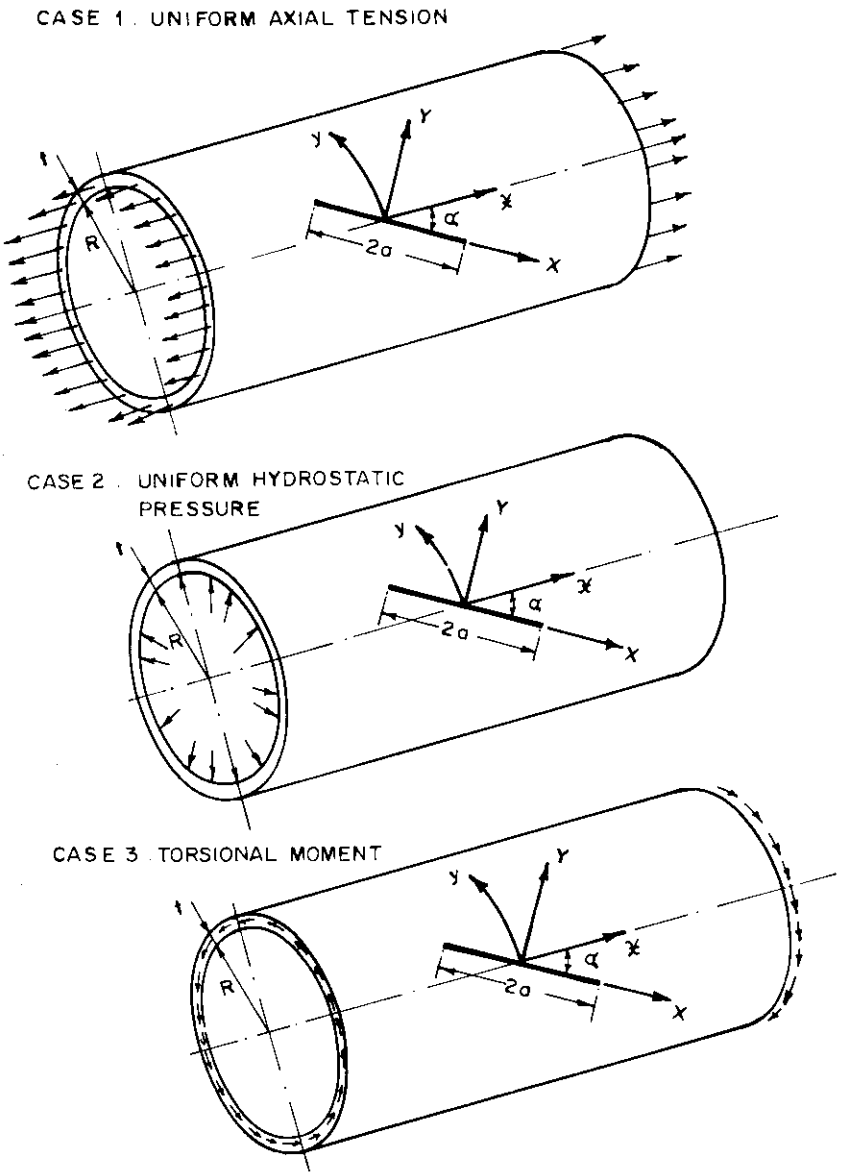

Figure 1. Configurations and loading conditions considered for analysis.

An elliptic coordinate system (ξ, η) is defined as follows:

$$X = \cosh \xi \cos \eta, \tag{3}$$

$$Y = \sinh \xi \sin \eta, \tag{4}$$

where the curves of $\xi =$ constant and $\eta =$ constant form an orthogonal system of confocal ellipses and hyperbolas with the common foci being the points $(X = \pm 1, Y = 0)$. The boundary of a straight crack is represented by $\xi = 0$.

We further define non-dimensional polar coordinates (r, θ) with a crack tip as the origin. These are related to (X, Y) by the following relations:

$$X = 1 + r \cos \theta \tag{5}$$

$$Y = r \sin \theta \tag{6}$$

TABLE I
Non-dimensionalising procedure

Nondimensional quantity	Symbol used	Non-dimensionalising factor
Coordinates	X, Y, x, y, r, K	a
Stress function	φ	$\sigma t a^2$
Normal displacement	W	$\sigma a^2[12(1-\nu^2)]^{1/2}/Et$
Stresses	$\sigma_\xi, \sigma_\eta, \tau_{\xi\eta}$	
	$\sigma_r, \sigma_\theta, \tau_{r\theta}$	σ
	$\sigma_x, \sigma_y, \tau_{xy}$	
	$\sigma_X, \sigma_Y, \tau_{XY}$	
Membrane forces	$N_\xi, N_\eta, N_{\xi\eta}$	
	$N_r, N_\theta, N_{r\theta}$	σt
Bending moments	$M_\xi, M_\eta, M_{\xi\eta}$	
	$M_r, M_\theta, M_{r\theta}$	$\sigma t^2/[12(1-\nu^2)]^{1/2}$
Transverse shear and Kirchoff shear forces	$Q_\xi, Q_\eta, \bar{Q}_\xi, \bar{Q}_\eta$	
	$Q_r, Q_\theta, \bar{Q}_r, \bar{Q}_\theta$	$\sigma t^2/a[12(1-\nu^2)]^{1/2}$
Stress intensity factors	$K_I^{(m)}, K_{II}^{(m)}, K_I^{(b)}, K_{II}^{(b)}$	$\sigma\sqrt{a}$
Laplacian Operator	∇^2	$1/a^2$

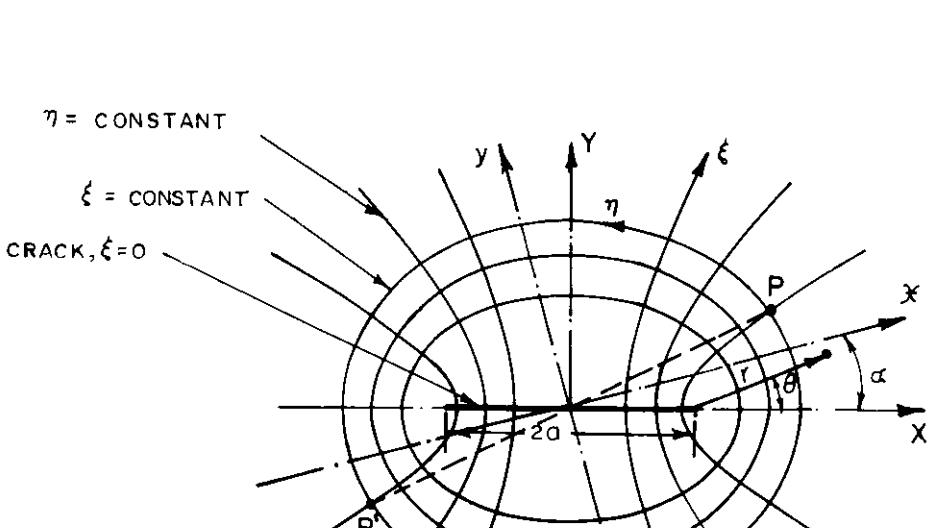

Figure 2. System of coordinates.

2.3. *Governing shell equation*

We define a "residual problem" as the problem of determining a stress field which, if superposed on the known state of stress in the shell in absence of the crack, gives the actual state of stress in the shell with the crack. Evidently, this stress field should arise from a system of self-equilibrating edge loads on the crack surface. In analysing the residual problem, these edge loads are determined from the condition that the crack surface should be stress-free in the final solution, and we take that part of the solution to governing shell equations, the stresses and displacements due to which vanish at infinity.

The governing differential equations used here are derived from the general shallow, thin shell equations given by Vlasov [7]. These can be reduced to a single, homogeneous equation for a dimensionless complex function $F = W - i\varphi$:

$$\nabla^2\nabla^2 F + 8i\beta^2 \frac{\partial^2 F}{\partial x^2} = 0, \tag{7}$$

where

$$\beta^2 = \frac{a^2}{8Rt}[12(1-\nu^2)]^{1/2} \tag{8}$$

$\nabla^2 = \left(\frac{\partial^2}{\partial x^2} + \frac{\partial^2}{\partial y^2}\right)$ in rectangular coordinates,

$\nabla^2 = \frac{1}{K^2}\left(\frac{\partial^2}{\partial \xi^2} + \frac{\partial^2}{\partial \eta^2}\right)$ in elliptic coordinates,

$K = [(\cosh 2\xi - \cos 2\eta)/2]^{1/2}$ is a non-dimensional scale factor for elliptic coordinates,

and R is the radius of the shell.

2.4. *Solutions to the governing shell equation*

We now seek solutions to the governing equation (7) keeping the following criteria in mind:

i) periodicity of the solution in η,
ii) symmetry considerations, and
iii) the condition that stresses and displacements vanish as $\xi \to \infty$.

We can write [8] the complete solution for (7) as follows:

$$F = \sum_{n=0,1,2,3,\ldots}^{\infty} (A_n + iB_n)F_n + \sum_{n=1,2,3,\ldots}^{\infty} (C_n + iD_n)F_n^* \tag{9}$$

where

$$F_{2j} = \cos[(1+i)\beta(\cos\alpha\cosh\xi\cos\eta + \sin\alpha\sinh\xi\sin\eta)]Me_{2j}^{(1)}(\xi, q)ce_{2j}(\eta, q) \tag{10}$$

$$F_{2j+1} = \sin[(1+i)\beta(\cos\alpha\cosh\xi\cos\eta + \sin\alpha\sinh\xi\sin\eta)]Me_{2j+1}^{(1)}(\xi, q)ce_{2j+1}(n, q) \tag{11}$$

$$F_{2j}^* = \cos[(1+i)\beta(\cos\alpha\cosh\xi\cos\eta + \sin\alpha\sinh\xi\sin\eta)]Ne_{2j}^{(1)}(\xi, q)se_{2j}(\eta, q) \tag{12}$$

$$F_{2j+1}^* = \sin[(1+i)\beta(\cos\alpha\cosh\xi\cos\eta + \sin\alpha\sinh\xi\sin\eta)]Ne_{2j+1}^{(1)}(\xi, q)se_{2j+1}(\eta, q) \tag{13}$$

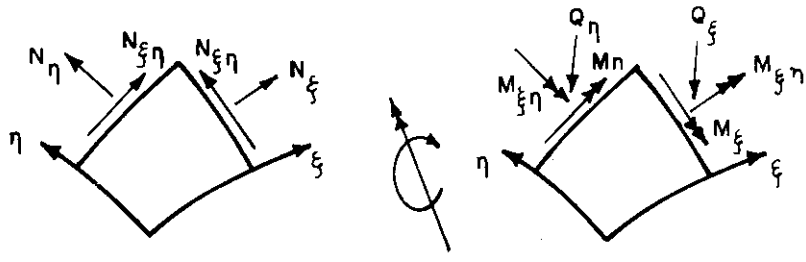

Figure 3. Stress resultants.

A_n, B_n, C_n and D_n are arbitrary real constants, notations followed for the Mathieu functions $se_n(\eta, q)$, $ce_n(\eta, q)$ and modified Mathieu functions $Me_n^{(1)}(\xi, q)$, $Ne_n^{(1)}(\xi, q)$ are identical with those of McLachlan [9], and q is a purely imaginary parameter given by

$$q = i\beta^2/2 \tag{14}$$

The non-dimensional stress resultants (Fig. 3) in elliptic coordinates can be expressed in terms of F[2]. Non-dimensional membrane and bending stresses can be obtained from these stress resultants using the relations given in [2].

3. Method of analysis — an outline

Solution to the governing shell equation is taken in the form of an infinite series as given in (9). The series is truncated to a specified number of terms and the arbitrary constants are evaluated by satisfying the crack surface boundary conditions using a collocation procedure. The next step is to transform the solution which is now completely determined, from elliptic to polar coordinates with a crack tip as the origin so as to recover the singular stresses in a convenient form. In the perturbation analysis presented in [1], such a transformation was carried out, term by term in the expanded form of W and φ. This method, if it is to be applied in the present approach, requires highly complicated logic in programming on the computer. The difficulty is overcome here by developing a method which involves expressing the solution through a Taylor series expansion around a crack tip and truncating it beyond terms which produce non-singular stresses. Computation of stress intensity factors then becomes a fairly simple process.

With the use of the conventional collocation procedure of satisfying the crack surface boundary conditions, it is found that convergence in results, in terms of stress intensity factors, is not satisfactory for certain cases. The difficulty is overcome by using a hybrid-collocation procedure. What we are doing is, in effect, equivalent to (i) satisfying the overall boundary conditions using the collocation procedure, and (ii) taking particular care of the singular stresses in the boundary conditions using power series expansions in the radial coordinate.

4. Computation of special functions

Effectiveness of the method of analysis outlined above depends to a large extent on the accuracy with which the Mathieu and modified Mathieu functions are evaluated numerically.

Methods of determination of characteristic numbers denoted by p in the Mathieu equation [9] are fairly well established for real values of q. A major difficulty in evaluating the Mathieu functions here arises from the fact that q, in the present problem is purely imaginary for which methods of computing p are not readily available. Power series expansions for p in terms of q, for q real or complex are available [9] but these extend only to a limited number of terms. Evidently these expansions are inaccurate for large values of β.

The power series expansions for p given by McLachlan [9] were obtained by taking the solution to the Mathieu equation as well as the characteristic numbers as power series in q. The condition of periodicity of the solution was then enforced in each term in its power series representation and this led to a progressive evaluation of successive terms in the power series for p in terms of q. In the present work, this analytical procedure was computerized by a matrix formulation and the power series for p is generated without any restriction on the number of terms.

For the computation of Mathieu functions, Fourier series expansions are used [9]. For the modified Mathieu functions the Bessel function product series, which is far more convergent than others, is used [9]. The characteristic coefficients which appear in the above series are determined from the well known recurrence formulae [9]. Derivatives of Mathieu and modified Mathieu functions are obtained by term wise differentiation of the series which is known to be valid [9].

5. Analysis of a cylindrical shell with an arbitrarily oriented crack

5.1. *Boundary conditions*

The residual problem in this case is defined by the following boundary conditions.

$$(N_\xi)_{\xi=0} = -(f_1 \sin^2\alpha + f_2 \cos^2\alpha + f_3 \sin 2\alpha), \tag{15}$$

$$(N_{\xi\eta})_{\xi=0} = (f_1 - f_2)\sin\alpha\cos\alpha + f_3 \cos 2\alpha, \tag{16}$$

$$(M_\xi)_{\xi=0} = 0 \tag{17}$$

$$(\tilde{Q}_\xi)_{\xi=0} = 0 \tag{18}$$

where the kirchoff shear $\tilde{Q}_\xi$ is given by

$$\tilde{Q}_\xi = Q_\xi + \frac{1}{K}\frac{\partial M_{\xi\eta}}{\partial \eta}$$

f_1, f_2 and f_3 are dimensionless load parameters the non-dimensionalising factor being σt. $f_1 = 1$, $f_2 = 0$, $f_3 = 0$ for loading by axial tension, $f_1 = 0$, $f_2 = 1$, $f_3 = 0$ for loading by internal pressure, and $f_1 = 0$, $f_2 = 0$, $f_3 = 1$ for loading by torsional moment.

5.2. *Numerical procedure*

The series solution (9) is truncated to a specified number of terms. The arbitrary real constants are determined from the criterion that the boundary conditions (15)–(18) be satisfied exactly at a specified number of points on the crack surface. If the number of points chosen is NP, the collocation points are located at $\eta = \frac{1}{2}\eta_{\text{INT}}, \frac{3}{2}\eta_{\text{INT}}, \frac{5}{2}\eta_{\text{INT}}, \ldots$ and

$(NP - \frac{1}{2})\eta_{INT}$, where $\eta_{INT} = \pi/NP$. For NP collocation points, NP terms are chosen in the series solution resulting in $4 * NP$ equations for $4 * NP$ unknowns. In the present work, the entire analytical process involved in generating and solving the linear algebraic equations for the unknown constants was computerised. The computation was started by taking the first ten terms in the series solution initially and increasing the number of terms in steps of two. The computation was terminated if less than 0.1% deviation was noticed in the stress intensity factors from two successive approximations.

5.3. *Transformation to polar coordinates*

With the arbitrary constants determined, the solution is completely known in elliptic coordinates. This solution is to be transformed to polar coordinates with a crack tip as the origin in order to recover the singular stresses and to evaluate the stress intensity factors. As we are interested here in the immediate vicinity of the crack tip, we carry out the transformation for $r \ll 1$. Also, as terms involving r^2 and higher powers of r in W and φ give rise to non-singular stresses, such terms are ignored. Accordingly, the trigonometric functions in (10)–(13) are expanded with the help of (3)–(6) as

$$\cos[(1+i)\beta(\cos\alpha\cosh\xi\cos\eta + \sin\alpha\sinh\xi\sin\eta)] = \lambda_1 - \lambda_2\mu_1 r\cos\theta - \mu_1\mu_2 r\sin\theta + 0(r^2) \tag{19}$$

$$\sin[(1+i)\beta(\cos\alpha\cosh\xi\cos\eta + \sin\alpha\sinh\xi\sin\eta)] = \mu_1 + \lambda_1\mu_2 r\sin\theta + \lambda_1\lambda_2 r\cos\theta + 0(r^2) \tag{20}$$

where

$$\lambda_1 = \cos[(1+i)\beta\cos\alpha] \tag{21}$$

$$\lambda_2 = (1+i)\beta\cos\alpha \tag{22}$$

$$\mu_1 = \sin[(1+i)\beta\cos\alpha] \tag{23}$$

$$\mu_2 = (1+i)\beta\sin\alpha \tag{24}$$

It now remains to transform the Mathieu and modified Mathieu functions in (10)–(13) to polar coordinates. It is to be noted that we need this transformation not over the entire domain, but only in the immediate vicinity of the crack tip and that in this zone, both the elliptic coordinates ξ and η are nearly zero. Since $\xi \simeq 0$ and $\eta \simeq 0$ in the region of interest, we carry out Taylor series expansions of the Mathieu and modified Mathieu functions around the crack tip defined by $\xi = \eta = 0$:

$$ce_n(\eta, q) = ce_n(0, q) + \frac{\eta}{\lambda}ce_n'(0, q) + \frac{\eta^2}{2\lambda}ce_n''(0, q) + \frac{\eta^3}{3\lambda}ce_n'''(0, q) + 0(\eta^4) \tag{25}$$

$$se_n(\eta, q) = se_n(0, q) + \frac{\eta}{\lambda}se_n'(0, q) + \frac{\eta^*}{2\lambda}se_n''(0, q) + \frac{\eta^3}{3\lambda}se_n'''(0, q) + 0(\eta^4) \tag{26}$$

$$Me_n(\xi, q) = Me_n(0, q) + \frac{\xi}{\lambda}Me_n'(0, q) + \frac{\xi^2}{2\lambda}Me_n''(0, q) + \frac{\xi^3}{3\lambda}Me_n'''(0, q) + 0(\xi^4) \tag{27}$$

$$Ne_n(\xi, q) = Ne_n(0, q) + \frac{\xi}{\lambda} Ne_n'(0, q) + \frac{\xi^2}{2\lambda} Ne_n''(0, q) + \frac{\xi^3}{3\lambda} Ne_n'''(0, q) + (\xi^4) \tag{28}$$

where

$$\xi = (2r)^{1/2} \cos\frac{\theta}{2} - \frac{1}{6\sqrt{2}} r^{3/2} \cos\frac{3\theta}{2} + 0(r^2) \tag{29}$$

$$\eta = (2r)^{1/2} \sin\frac{\theta}{2} - \frac{1}{6\sqrt{2}} r^{3/2} \sin\frac{3\theta}{2} + 0(r^2) \tag{30}$$

$\dot{(\ )}$ and $(\ )'$ denote differentiation with respect to η and ξ respectively. Superscript (1) is omitted in $Me_n(\xi, q)$ and $Ne_n(\xi, q)$ for the sake of brevity. Terms involving fourth and higher powers of ξ and η are dropped in (25)–(28) as ξ and η given by (29)–(30) are of order $r^{1/2}$. From the Fourier series expansions for the Mathieu functions [9], it follows that

$$ce_n(0, q) = \dot{ce}_n(0, q) = se_n(0, q) = \dot{se}_n(0, q) = 0 \tag{31}$$

From the properties of Mathieu and modified Mathieu functions, it can be shown that

$$Me_n(0, q)\dot{ce}_n(0, q) + Me_n''(0, q)ce_n(0, q) = 0 \tag{32}$$

Using (19)–(32), the general term in the series solution defined by (10)–(13) can be expressed in terms of (r, θ) as follows:

$$\begin{aligned}
F_{2j} = {} & \lambda_1 Me_{2j}(0, q)ce_{2j}(0, q) \\
& + [\sqrt{2}\lambda_1 Me_{2j}'(0, q)ce_{2j}(0, q)]r^{1/2}\cos\frac{\theta}{2} \\
& + [\lambda_1 Me_{2j}''(0, q)ce_{2j}(0, q) \\
& - \lambda_2\mu_1 Me_{2j}(0, q)ce_{2j}(0, q)]r\cos\theta \\
& + \left[\frac{1}{2\sqrt{2}}\{Me_{2j}'''(0, q)ce_{2j}(0, q) + Me_{2j}'(0, q)\dot{ce}_{2j}(0, q)\}\right. \\
& \left. - \frac{\lambda_2\mu_1}{\sqrt{2}} Me_{2j}'(0, q)ce_{2j}(0, q)\right]r^{3/2}\cos\frac{\theta}{2} \\
& + \left[\frac{\lambda_1}{6\sqrt{2}}\{Me_{2j}'''(0, q)ce_{2j}(0, q) - Me_{2j}'(0, q)\dot{ce}_{2j}(0, q)\}\right. \\
& - \frac{\lambda_1}{2\sqrt{2}} Me_{2j}'(0, q)\dot{ce}_{2j}(0, q) \\
& \left. - \frac{\lambda_2\mu_1}{\sqrt{2}} Me_{2j}'(0, q)ce_{2j}(0, q)\right]r^{3/2}\cos\frac{3\theta}{2} \\
& + [-\mu_1\mu_2 Me_{2j}(0, q)ce_{2j}(0, q)]r\sin\theta \\
& + \left[-\frac{\mu_1\mu_2}{\sqrt{2}} Me_{2j}'(0, q)ce_{2j}(0, q)\right]r^{3/2}\sin\theta/2 \\
& + \left[-\frac{\mu_1\mu_2}{\sqrt{2}} Me_{2j}'(0, q)ce_{2j}(0, q)\right]r^{3/2}\sin\frac{3\theta}{2} \\
& + 0(r^2)
\end{aligned} \tag{33}$$

$$
\begin{aligned}
F_{2j+1} = {} & \mu_1 Me_{2j+1}(0, q)ce_{2j+1}(0, q) \\
& + [\sqrt{2}\mu_1 M'_{2j+1}(0, q)ce_{2j+1}(0, q)]r^{1/2}\cos\frac{\theta}{2} \\
& + [\mu_1 Me''_{2j+1}(0, q)ce_{2j+1}(0, q) \\
& + \lambda_1\lambda_2 Me_{2j+1}(0, q)ce_{2j+1}(0, q)]r\cos\theta \\
& + \left[\frac{\mu_1}{2\sqrt{2}}\{Me'''_{2j+1}(0, q)ce_{2j+1}(0, q) + Me'_{2j+1}(0, q)ce'_{2j+1}(0, q)\}\right. \\
& \left. + \frac{\lambda_1\lambda_2}{\sqrt{2}} Me'_{2j+1}(0, q)ce_{2j+1}(0, q)\right]r^{3/2}\cos\frac{\theta}{2} \\
& + \left[\frac{\mu_1}{6\sqrt{2}}\{Me'''_{2j+1}(0, q)ce_{2j+1}(0, q) - Me'_{2j+1}(0, q)ce_{2j+1}(0, q)\}\right. \\
& - \frac{\mu_1}{2\sqrt{2}} Me'_{2j+1}(0, q)ce'_{2j+1}(0, q) \\
& \left. + \frac{\lambda_1\lambda_2}{\sqrt{2}} Me'_{2j+1}(0, q)ce_{2j+1}(0, q)\right]r^{3/2}\cos\frac{3\theta}{2} \\
& + [\lambda_1\mu_2 Me_{2j+1}(0, q)ce_{2j+1}(0, q)]r\sin\theta \\
& + \left[\frac{\lambda_1\mu_2}{\sqrt{2}} Me'_{2j+1}(0, q)ce_{2j+1}(0, q)\right]r^{3/2}\sin\frac{\theta}{2} \\
& + \left[\frac{\lambda_1\mu_2}{\sqrt{2}} Me'_{2j+1}(0, q)ce_{2j+1}(0, q)\right]r^{3/2}\sin\frac{3\theta}{2} \\
& + 0(r^2)
\end{aligned}
$$

$$
\begin{aligned}
F^*_{2j} = {} & [\sqrt{2}\lambda_1 Ne_{2j}(0, q)se'_{2j}(0, q)]r^{1/2}\sin\frac{\theta}{2} \\
& + [\lambda_1 Ne'_{2j}(0, q)se'_{2j}(0, q)]r\sin\theta \\
& + \left[\frac{\lambda_1}{2\sqrt{2}} Ne_{2j}(0, q)se''_{2j}(0, q)\right. \\
& + \frac{\lambda_2\mu_1}{\sqrt{2}} Ne_{2j}(0, q)se'_{2j}(0, q) \\
& \left. + \frac{\lambda_1}{2\sqrt{2}} Ne''_{2j}(0, q)se'_{2j}(0, q)\right]r^{3/2}\sin\frac{\theta}{2} \\
& + \left[-\frac{\lambda_1}{6\sqrt{2}} Ne_{2j}(0, q)\{se'_{2j}(0, q) + se'''_{2j}(0, q)\}\right. \\
& - \frac{\lambda_2\mu_1}{\sqrt{2}} Ne_{2j}(0, q)se'_{2j}(0, q) \\
& \left. + \frac{\lambda_1}{2\sqrt{2}} Ne''_{2j}(0, q)se'_{2j}(0, q)\right]r^{3/2}\sin\frac{3\theta}{2} \\
& + \left[-\frac{\mu_1\mu_2}{\sqrt{2}} Ne_{2j}(0, q)se'_{2j}(0, q)\right]r^{3/2}\cos\frac{\theta}{2} \\
& + \frac{\mu_1\mu_2}{\sqrt{2}} Ne_{2j}(0, q)se'_{2j}(0, q)\Big]r^{3/2}\cos\frac{3\theta}{2} + 0(r^2)
\end{aligned}
$$

$$
\begin{aligned}
F^*_{2j+1} = {} & [\sqrt{2}\mu_1 Ne_{2j+1}(0, q)se'_{2j+1}(0, q)]r^{1/2}\sin\frac{\theta}{2} \\
& + [\mu_1 Ne'_{2j+1}(0, q)se'_{2j+1}(0, q)]r\sin\theta \\
& + \left[\frac{\mu_1}{2\sqrt{2}} Ne_{2j+1}(0, q)se''_{2j+1}(0, q)\right. \\
& - \frac{\lambda_1\lambda_2}{2\sqrt{2}} Ne_{2j+1}(0, q)se'_{2j+1}(0, q) \\
& \left. + \frac{\mu_1}{2\sqrt{2}} Ne''_{2j+1}(0, q)se'_{2j+1}(0, q)\right]r^{3/2}\sin\frac{\theta}{2} \\
& + \left[-\frac{\mu_1}{6\sqrt{2}} Ne_{2j+1}(0, q)\{se'_{2j+1}(0, q) + se'''_{2j+1}(0, q)\}\right. \\
& + \frac{\lambda_1\lambda_2}{\sqrt{2}} Ne_{2j+1}(0, q)se'_{2j+1}(0, q) \\
& \left. + \frac{\mu_1}{2\sqrt{2}} Ne''_{2j+1}(0, q)se'_{2j+1}(0, q)\right]r^{3/2}\sin\frac{3\theta}{2} \\
& + \left[\frac{\lambda_1\mu_2}{\sqrt{2}} Ne_{2j+1}(0, q)se'_{2j+1}(0, q)\right]r^{3/2}\cos\frac{\theta}{2} \\
& + \left[-\frac{\lambda_1\mu_2}{\sqrt{2}} Ne_{2j+1}(0, q)se'_{2j+1}(0, q)\right]r^{3/2}\cos\frac{3\theta}{2} \\
& + 0(r^2)
\end{aligned}
\tag{36}
$$

Evaluation of F_{2j}, F_{2j+1}, F^*_{2j} and F^*_{2j+1} from the foregoing equations is fairly simple from the computational point of view, because the modified Mathieu functions and their derivatives at $\xi = 0$ are already evaluated during the process of satisfying the boundary conditions. Mathieu functions and their derivatives at $\eta = 0$ are easily evaluated from their Fourier series expansions. Solution for the complex stress-displacement function F is obtained in polar coordinates by substituting Eqns. (33)–(36) in (9) and carrying out the summation. This is done on the computer as the arbitrary constants A_n, B_n, C_n and D_n are already evaluated. Separating the real and imaginary parts, we get the stress function $\phi(r, \theta)$ and normal displacement $W(r, \theta)$ in the form:

$$
\begin{aligned}
\phi = {} & \Phi_0 + \Phi_1 r^{1/2}\cos\frac{\theta}{2} + \Phi_2 r\cos\theta + \Phi_3 r^{3/2}\cos\frac{\theta}{2} \\
& + \Phi_4 r^{3/2}\cos\frac{3\theta}{2} + \Phi_5 r^{1/2}\sin\frac{\theta}{2} + \Phi_6 r\sin\theta + \Phi_7 r^{3/2}\sin\frac{\theta}{2} \\
& + \phi_8 r^{3/2}\sin\frac{3\theta}{2} + 0(r^2)
\end{aligned}
\tag{37}
$$

$$
\begin{aligned}
W = {} & W_0 + W_1 r^{1/2}\cos\frac{\theta}{2} + W_2 r\cos\theta + W_3 r^{3/2}\cos\frac{\theta}{2} + W_4 r^{3/2}\cos\frac{3\theta}{2} \\
& + W_5 r^{1/2}\sin\frac{\theta}{2} + W_6 r\sin\theta + W_7 r^{3/2}\sin\frac{\theta}{2} + W_8 r^{3/2}\sin\frac{3\theta}{2} + 0(r^2)
\end{aligned}
\tag{38}
$$

where Φ_j, W_j ($j = 0$ to 8) are obtained as numerical values from the computer.

Non-dimensional stress resultants and stresses in polar coordinates can be determined from (37)–(38) using the relations given in [2].

A simple check on the computer values of Φ_j, W_j ($j = 0$ to 8) is to confirm that the following crack surface boundary conditions reformulated in polar coordinates are satisfied:

$$N_\theta = -(f_1 \sin^2 \alpha + f_2 \cos^2 \alpha + f_3 \sin 2\alpha),$$

$$N_{r\theta} = (f_1 - f_2) \sin \alpha \cos \alpha + f_3 \cos 2\alpha,$$

$$M_\theta = 0,$$

$$\tilde{Q}_\theta = Q_\theta + \frac{\partial M_{r\theta}}{\partial \theta} = 0, \text{ along } \theta = \pm \pi.$$

using (37)–(38) to satisfy the foregoing boundary conditions and satisfying the resulting equations term by term in the power series in $r^{1/2}$, we get

$$\Phi_1 = 0 \tag{39}$$

$$\Phi_3/\Phi_4 = 3 \tag{40}$$

$$\Phi_5 = 0 \tag{41}$$

$$\Phi_7/\Phi_8 = 1 \tag{42}$$

$$W_1 = 0 \tag{43}$$

$$W_3/W_4 = 3(\nu - 1)/(7 + \nu) \tag{44}$$

$$W_5 = 0 \tag{45}$$

$$W_7/W_8 = 3(\nu - 1)/(5 + 3\nu) \tag{46}$$

5.4. *Determination of stress intensity factors*

Following the convention for flat plates, we define mode I and mode II components of membrane and bending stress intensity factors as follows:

$$\sigma_\theta^{(m)}(r, \theta = 0) = \frac{K_I^{(m)}}{\sqrt{2r}} + 0(r^0) \tag{47}$$

$$\sigma_\theta^{(b)}(r, \theta = 0) = \frac{K_I^{(b)}}{\sqrt{2r}} + 0(r^0) \tag{48}$$

$$\tau_{r\theta}^{(m)}(r, \theta = 0) = \frac{K_{II}^{(m)}}{\sqrt{2r}} + 0(r^0) \tag{49}$$

$$\tau_{r\theta}^{(b)}(r, \theta = 0) = \frac{K_{II}^{(b)}}{\sqrt{2r}} + 0(r0) \tag{50}$$

where the superscripts (m) and (b) refer to membrane and bending stresses and the subscripts I and II refer to mode I and mode II components. It may be recalled that the stress intensity factors $K_I^{(m)}$, $K_I^{(b)}$, $K_{II}^{(m)}$, $K_{II}^{(b)}$ are non-dimensionalised with respect to $\sigma\sqrt{a}$. Using (37)–(38), these stress intensity factors are obtained as simple algebraic expressions:

$$K_I^{(m)} = 3(\Phi_3 + \Phi_4)/2\sqrt{2} \tag{51}$$

$$K_{II}^{(m)} = -(\Phi_7 + 3\Phi_8)/2\sqrt{2} \tag{52}$$

$$K_I^{(b)} = 3[3(1 - \nu)W_4 - (5 + 3\nu)W_3]/[24(1 - \nu^2)]^{1/2} \tag{53}$$

$$K_{II}^{(b)} = 3(\nu - 1)[W_7 + 3W_8]/[24(1 - \nu^2)]^{1/2} \tag{54}$$

Distribution of singular stresses in the vicinity of the crack tip in terms of these stress intensity factors is then obtained in the usual form [1, 8].

5.5. *Computational errors and convergence*

The test of convergence during computations was applied on the total stress intensity factor $K_{\mathrm{I}}^{(\mathrm{tot})}$ or $K_{\mathrm{II}}^{(\mathrm{tot})}$ given by

$$K_{\mathrm{I}}^{(\mathrm{tot})} = K_{\mathrm{I}}^{(\mathrm{m})} + K_{\mathrm{I}}^{(\mathrm{b})}$$

$$K_{\mathrm{II}}^{(\mathrm{tot})} = K_{\mathrm{II}}^{(\mathrm{m})} + K_{\mathrm{II}}^{(\mathrm{b})}.$$

Numerical results showed satisfactory convergence in general except for some combinations of β and α. We thus find that the collocation procedure, in spite of its proven effectiveness in satisfying the overall boundary conditions, cannot handle the mathematical limiting process in the vicinity of crack tips for such cases. Obviously modifications would be necessary in our numerical procedure for these combinations of β and α. We shall now study this aspect.

We look back at (39)–(46) which are obtained by reformulating the crack surface boundary conditions in polar coordinates. These equations serve also as a useful check on mathematical formulation of the problem, the correctness of computer programming, and computational errors such as round-off etc. Numerical results show that convergence is assured whenever these equations are clearly satisfied. Convergence is not satisfactory when (39)–(46) are not satisfied. So, one concludes that the mathematical formulation and computer programming are faultless, but the computational errors over power the solution in certain cases. The values of β and α for which this happens is obviously not unique but depends on computer limitations and programming details.

A closer look at the origin of (39)–(46) shows that they actually represent boundary conditions on singular stresses in the vicinity of the crack tip. Therefore, these can be enforced as additional conditions to be satisfied during the evaluation of the arbitrary constants. that means, if the first NT terms are considered in the series solution (9) resulting in $4 * \mathrm{NT}$ unknowns, eight of the $4 * \mathrm{NT}$ equations required are derived from (39)–(46) while the remaining $(4 * \mathrm{NT}\text{-}8)$ equations are derived by satisfying the boundary conditions (15)–(18) at (NT-2) collocation points. Hence, the technique we use is in a sense, of a hybrid type and is found to result in excellent convergence over the range β and α considered.

5.6. *Discussion of results*

The distribution patterns of the membrane and bending stresses in the vicinity of the crack tip obtained in the present analysis [8] are identical with the perturbation solution given in [1] and the plate solutions for the cases of extension [10] and bending [11]. We therefore conclude that, irrespective of the size and orientation of the crack, the distribution patterns of the membrane and bending stresses in the vicinity of the crack tip for the cylindrical shell are identical with those found in plates both with regard to the inverse square root singularity in r and angular distribution in the θ coordinate. Curvature has only the effect of increasing the intensity of the singular stresses. This is in agreement with conclusions drawn in earlier works on symmetrically oriented cracks.

Results from the present analysis suggest that the angular distribution of membrane stresses is independent of the Poisson's ratio whereas this is not true of bending

stresses. Analysis of a pressurized cylindrical shell with an axial crack by Krenk [12] and with a circumferential crack by Delale and Erdogan [13] from Reissner's theory shows that the order of singularity of membrane and bending stresses near the crack tip agrees with predictions from classical shallow thin shell theory but the angular distribution of bending stresses is independent of ν and is exactly identical with the one for membrane stresses. One could therefore expect that similar investigation of the present problem by a tenth order shell theory might lead to the same conclusion.

In view of the range of problems covered in the analysis and also as the number of parameters involved is large, non-dimensional stress intensity factors are presented and discussed only for the pressure loading case. But the computer program developed can be readily used to generate the results for the other two loading cases.

It is clear from the general formulation that the problem for the loading case considered is completely defined by the three- non-dimensional parameters β and α, and ν. Numerical calculations in this paper were performed on an IBM 370/155 computer using double precision arithmetic. Results were obtained for $\nu = 0.3$, in terms of β and α in the ranges $0 \leqslant \beta \leqslant 1.2$ and $0 \leqslant \alpha \leqslant 90°$.

Comparison with earlier theoretical solutions. For a pressurised cylindrical shell with an axial crack, we shall first compare results from the present analytical-numerical procedure with those from [2]. Table 2 gives a comparison of mode I membrane and bending stress intensity factors for $\alpha = 0$ and $0 \leqslant \beta \leqslant 1.2$. As the comparison shows, the boundary collocation procedure employed in the present analysis and the Fourier series formulation used by Murthy *et al.* [2] give identical results. Incidentally, this comparison has also served to provide useful check against errors in programming the present method of analysis on the computer. Figures 4 and 5 show the variation of mode I membrane and bending stress intensity factors with the curvature parameter β. The figures also show the perturbation solutions taken from [1] but we will defer discussion on this to a later stage. Variation of $K_I^{(m)}$ is parabolic for small values of β and approximately linear for higher values of β. $K_I^{(b)}$ increases with β, reaches a maximum value and starts decreasing with further increase in β. These trends in the behaviour of $K_I^{(m)}$ and $K_I^{(b)}$ are in agreement with the earlier works.

Comparison with perturbation solutions. We shall now compare results from the present analytical-numerical method with those from the perturbation analysis presented in [1]. Table 3 gives a comparison of stress intensity factors $K_I^{(m)}$, $K_I^{(b)}$, $K_{II}^{(m)}$

TABLE II

Comparison of results from the present analysis with earlier solutions

Configuration and loading: Pressurised cylindrical shell with an axial crack. [$\alpha = 0$, $\nu = 0.3$]

	Mode I Membrane SIF $K_I^{(m)}$		Mode I Bending SIF $K_I^{(b)}$	
Curvature Parameter β	Present analysis	Ref. [2]	Present analysis	Ref. [2]
0.0	1.0	1.0	0.0	0.0
0.2	1.071	1.07	0.101	0.101
0.4	1.245	1.245	0.219	0.219
0.6	1.476	1.476	0.305	0.305
0.8	1.737	1.737	0.354	0.354
1.0	2.011	2.011	0.371	0.371
1.2	2.288	2.288	0.358	0.358

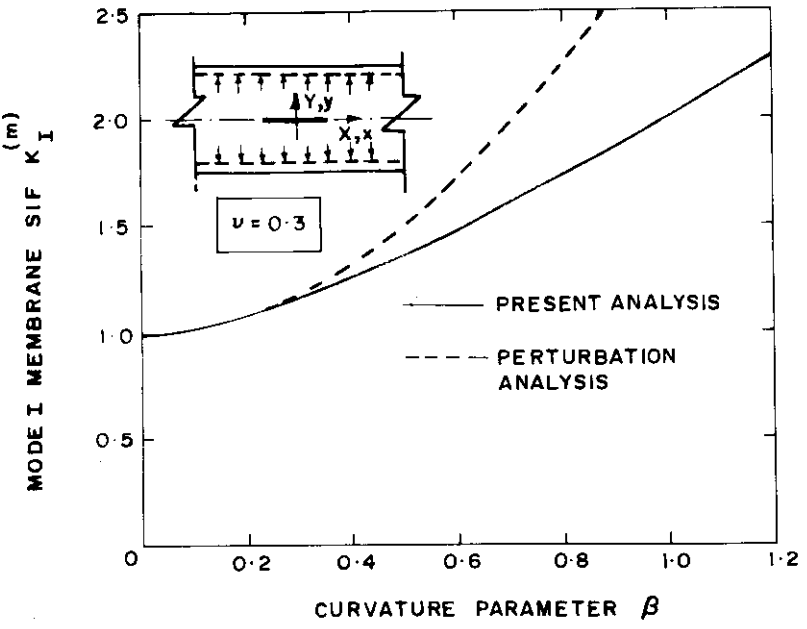

Figure 4. Mode I Membrane SIF for an axial crack in a pressurised cylindrical shell plotted as a function of β.

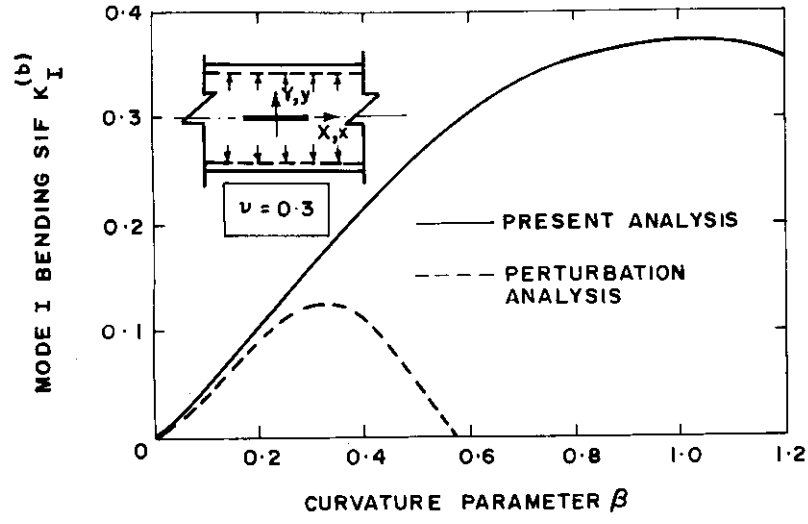

Figure 5. Mode I bending SIF for an axial crack in a pressurised cylindrical shell plotted as a function β.

and $K_{II}^{(b)}$ obtained by the two methods for $\beta = 0.2$ and $0 \leq \alpha \leq 90°$. As the comparison shows, the perturbation analysis does prove to be almost exact for this value of β. Incidentally, this comparison has also provided a check against errors in lengthy algebraic work carried out in the perturbation analysis. A comparison of perturbation solutions with the present analytical-numerical results over a wide range of β for $\alpha = 0$ is shown in Figs. 4 and 5. It is seen that as β increases, the difference in membrane stress intensity factor is not large but the error in perturbation solution arises mainly from the bending stress intensity factor. It is also evident from Fig. 5 that $K_I^{(b)}$ will reverse sign but the value of β at which this happens is far higher than

TABLE III

Comparison of results from the present analysis with perturbation solutions for a pressurised cylindrical shell with arbitrarily oriented cracks [$\beta = 0.2$, $\nu = 0.3$]

	Mode I Membrane SIF $K_I^{(m)}$		Mode I Bending SIF $K_I^{(b)}$		Mode II Membrane SIF $K_{II}^{(m)}$		Mode II Bending SIF $K_{II}^{(b)}$	
α (Degrees)	Present Analysis	Perturbation Solution [1]	Present Analysis	Perturbation Solution [1]	Present Analysis	Perturbation Solution [1]	Present Analysis	Perturbation Solution [1]
0	1.071	1.078	0.101	0.091	0.0	0.0	0.0	0.0
10	1.041	1.045	0.092	0.091	0.173	0.178	0.007	0.007
20	0.943	0.949	0.100	0.088	0.327	0.335	0.012	0.012
30	0.798	0.803	0.093	0.084	0.441	0.450	0.012	0.012
40	0.622	0.625	0.079	0.074	0.504	0.504	0.008	0.008
50	0.438	0.438	0.060	0.058	0.503	0.506	0.002	0.002
60	0.264	0.264	0.038	0.038	0.442	0.443	−0.002	−0.002
70	0.123	0.123	0.019	0.019	0.327	0.327	−0.004	−0.005
80	0.031	0.032	0.005	0.005	0.173	0.174	−0.003	−0.003
90	0.0	0.0	0.0	0.0	0.0	0.0	0.0	0.0

that predicted by the perturbation analysis. Thus, the perturbation solution gives an erroneous prediction of the critical shell surface on which fracture is initiated under static loads beyond a certain value of β. A similar comparison of perturbation solutions and analytical-numerical results for all other values of α shows that the perturbation solution can be considered to be valid for β upto 0.5 if errors upto 5% could be admitted.

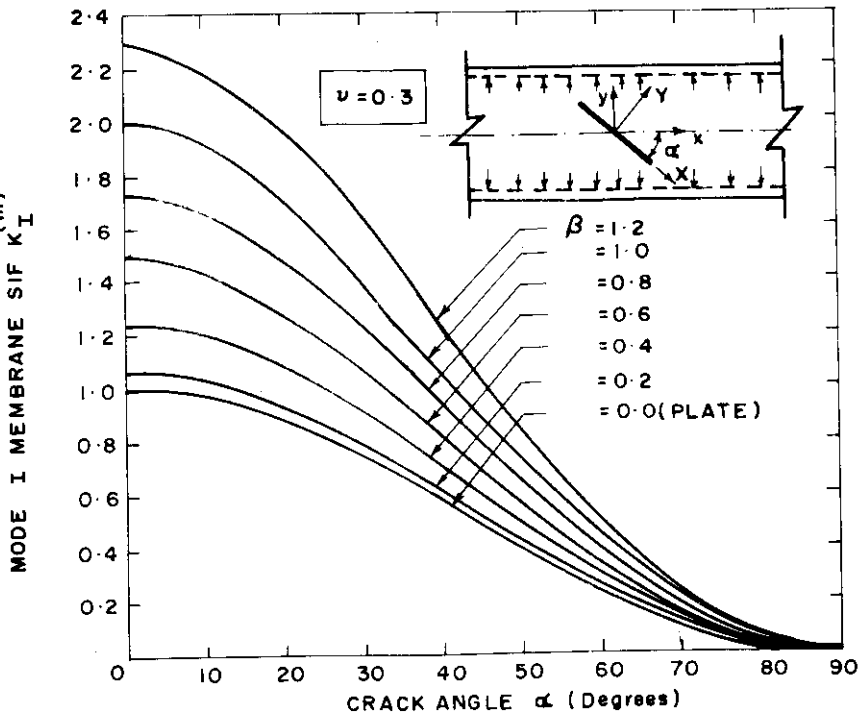

Figure 6. Mode I membrane SIF for an arbitrarily oriented crack in a pressurised cylindrical shell plotted as a function of β.

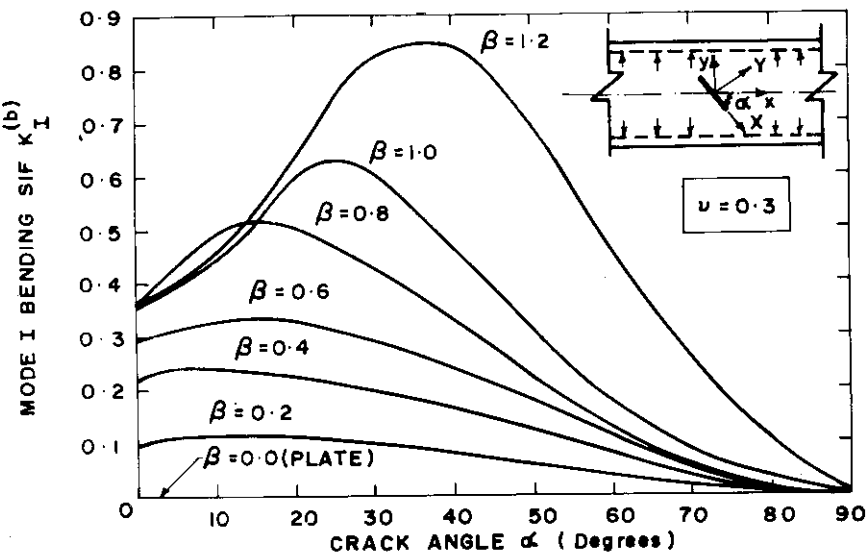

Figure 7. Mode I bending SIF for an arbitrarily oriented crack in a pressurised cylindrical shell plotted as a function of β.

Parametric study. A parametric study of the stress intensity factors with respect to α and β for $\nu = 0.3$ is shown in Figs. 6 to 9. It can be seen that

(i) The peak value of the mode I membrane stress intensity factor $K_{\mathrm{I}}^{(m)}$ is always reached at $\alpha = 0$ and its magnitude increases with β.

(ii) Mode I bending stress intensity factor $K_{\mathrm{I}}^{(b)}$ becomes quite significant for higher values of β.

(iii) The magnitude of the mode II membrane stress intensity factor also increases with β for all values of α (other than 0° and 90° for which it is zero). However, as β increases, the departure from the plate solution is not large. Similar observations are valid for the mode II bending stress intensity factor $K_{\mathrm{II}}^{(b)}$.

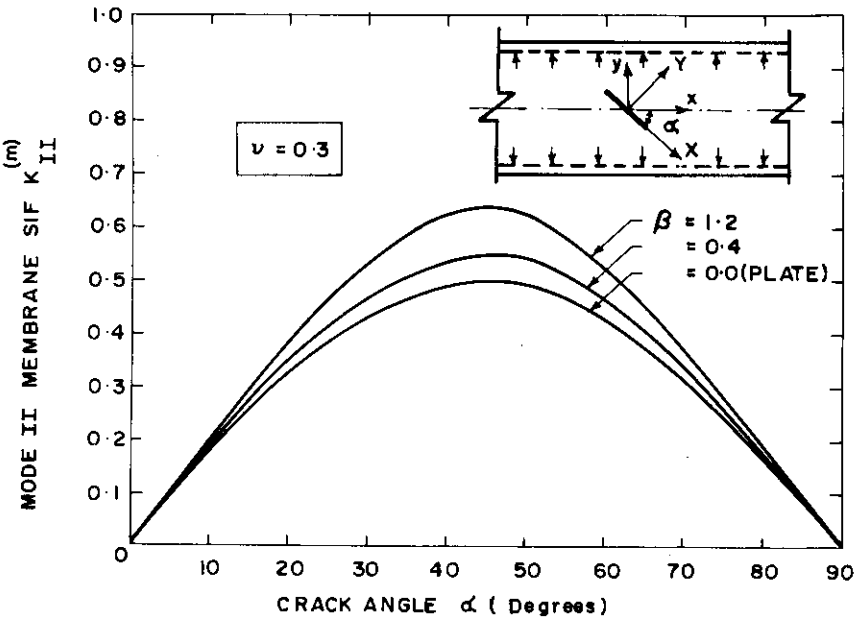

Figure 8. Mode II membrane SIF for an arbitrarily oriented crack in a pressurised cylindrical shell plotted as a function of β.

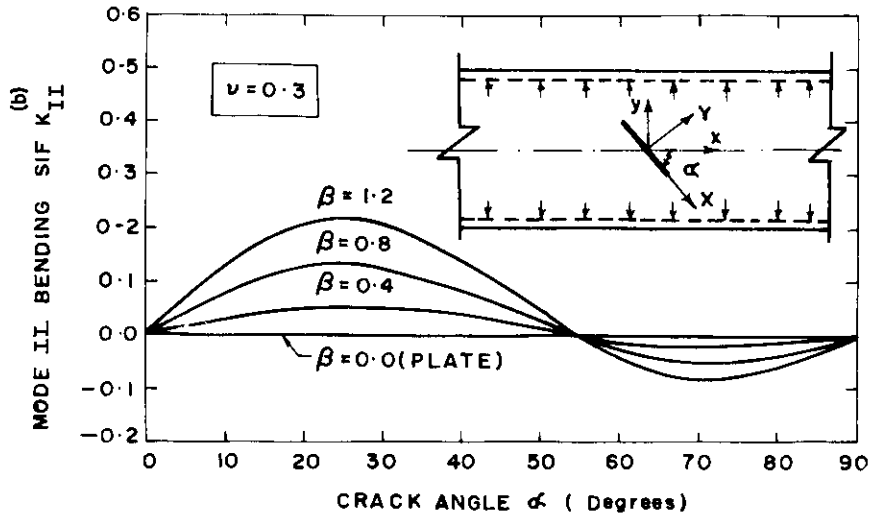

Figure 9. Mode II bending SIF for an arbitrarily oriented crack in a pressurised cylindrical shell plotted as a function of β.

6. Concluding remarks

In this paper, we have presented an analytical-numerical procedure for the determination of membrane and bending stress intensity factors for an arbitrarily oriented crack in a cylindrical shell. The work is a logical extension of the perturbation analysis to cover a wide practical range of the parameters involved. Mathematical formulation and computational details needed for this analysis are also given. Numerical results are presented for the pressure loading case to show the evidence to the conclusion that the proposed method of analysis has satisfactory convergence and accuracy over a wide range of the parameters involved.

The method of analysis presented in this paper should be of special interest in the light of techniques used earlier for such problems. Crack problems in shells have been treated in the past mainly by integral equation methods whereas, here, the problem is solved from the differential equation approach of particular interest should be the hybrid-collocation technique used for satisfying the crack surface boundary conditions and the Taylor series expansion used to transform the solution from elliptic to polar coordinates.

REFERENCES

[1] H.V. Lakshminarayana and M. V. V. Murthy, *International Journal of Fracture* 12 (1976) 547–566.
[2] M.V.V. Murthy, A.K. Rao and K.P. Rao, *International Journal of Solids and Structures* 10 (1974) 1243–1269.
[3] *Mechanics of Fracture*, Vol. 3, ed. G.C. Sih, Noordhoff International Publishing, Leyden (1977).
[4] E.S. Folias, *International Journal of Fracture Mechanics* 5 (1969) 327–346.
[5] J.G. Simmonds, M. R. Bradley and J.W. Nicholson, *Journal of Applied Mechanics* 45 (1978) 135–141.
[6] P.D. Ewing and J.G. Williams, *International Journal of Fracture* 10 (1974) 537–544.
[7] V.Z. Vlasov, *General Theory of Shells and its Applications in Engineering*, NASA Technical Translation, NASA TT F-99, April 1964.
[8] H.V. Lakshminarayana, Ph.D. Thesis, Indian Institute of Science, Bangalore, India (1980).
[9] N.W. McLachlan, *Theory and Application of Mathieu Functions*, Oxford University Press (1951).
[10] M.L. Williams, *Journal of Applied Mechanics* 24 (1957) 109–114.
[11] M.L. Williams, *Journal of Applied Mechanics* 28 (1961) 78–82.
[12] S. Krenk, *International Journal of Fracture* 14 (1978) 123–143.
[13] F. Delale and F. Erdogan, *Quarterly of Applied Mathematics* 37 (1979) 239–258.